SoftTouch: A Sensor-Placement Framework for Soft Robotic Hands

Chao Li[1] and Nancy Pollard[2]

Abstract— **Sensor placement for grasping tasks in conventional robotic hands has been extensively studied, with goals including sensorizing essential contact areas or determining the effect of number of sensors on performance. However, with the new generation of dexterous soft robotic hands that deform to the shape of the object, the former frameworks may not be sufficient. In particular, we find that real-world experiments are essential to determine the value of different sensors and the effect of different sensor placements due to the complex interactions between the deformable robot body, sensor material properties, and sensor and task performance. In this paper, we propose a sensor-placement framework for dexterous soft robotic hands that is easily reconfigurable to different hand designs using off-the-shelf sensors. Our three-step framework selects and evaluates candidate sensor configurations to determine the effectiveness of sensors in each configuration for estimating qualitative and quantitative manipulation metrics. We tested our framework on a soft robotic hand to select the optimum sensor placement for a given set of manipulation patterns using force and inertial sensors. Our studies show that sensors placed at contact points are best for predicting the qualitative success of the manipulation. However, when it comes to estimating quantitative manipulation metrics, off-the-shelf sensors placed at contact points decrease performance for some manipulation types. This performance decrease may be due to the disturbance they create to surface texture, deformation patterns, and weight of soft robotic systems.**

I. Introduction

Sensor placement for conventional rigid robotic hands is an extensively researched topic [1], [2], with approaches ranging from contact-based to mathematical-based. These frameworks seek to optimize sensor placement so that we can better understand the interactions between the object and the hand during contact. Many of these studies concluded that sensors should be placed at contact locations, forming the sensor placement framework for many robotic hands [3].

However, there has been a new generation of soft [4]–[8], and dexterous [8]–[10] robotic hands. These new hands exhibit different physical characteristics compared to conventional rigid systems [11]. In particular, soft robotic hands deform more than conventional rigid hands when they interact with objects [9], [10]. Since the whole hand is one piece of deformable material, large vibrations pass through the hand differently and can even be propagated to the entire hand. Therefore, precise contact points can be measured not just at the fingertips but also along the length and side of the fingers and inside the palm [12].

[1]Chao Li is with the Department of Electrical and Computer Engineering, Carnegie Mellon University, Pittsburgh, PA, 15213, USA chaoli2@cmu.edu

[2]Nancy Pollard is with the faculty at the Robotics Institute, School of Computer Science, Carnegie Mellon University, Pittsburgh, PA, 15213, USA npollard@cmu.edu

Moreover, the way that sensors interact with the object in the soft hand can be different from rigid hands. Given that the soft hand deforms to the shape of the object [13], the sensors must be able to adapt with the deformity of the hand. Off-the-shelf force sensors placed at contact locations tend to be rigid [12]. Therefore, the redistribution of the forces caused by the difference in compliance of these sensors and the soft hand during the interaction could corrupt the sensors' data. The difference in texture of these sensors can also affect the grip between the object and the soft hand, therefore affecting the quality of the manipulation.

Furthermore, little work has been done on perceptual methods and their relationship to dexterous robotic manipulation [14]. The signals that are picked up by the sensors during a dexterous manipulation are different from conventional grasping tasks. This is because for a fully autonomous hand, the sensors must be able to track the progress of the manipulation in addition to sensing contact. Therefore, an ideal sensor placement should pick up both these signals to reveal the quality of the manipulation. While the motion of the dexterous manipulation can be tracked using optical methods, high frequencies of slip makes it difficult for camera to capture [12]. Visual cameras can also be difficult to use because of occlusions that occur during the manipulation [15]. Therefore, more studies are needed to develop hardware for processing tactile information in conjunction with vision.

A good sensor placement for soft and dexterous hands can help address the challenging task to develop fully autonomous soft robotic hands capable of achieving or exceeding human-level dexterity [14]. Effective autonomous dexterous manipulation requires sensor perception that accurately estimates state or knows the surrounding environment [9], [16], [17]. Sensor placement can affect the quality of the data received and therefore the next state decisions made by the system [13]. The signals received from a good sensor placement can also help us to better understand the interactions between the soft robotic hand and the object during the dexterous manipulation. This allows researchers to calculate more stable interaction states between the hand and the object on a physical robotic hand [18].

In this paper, we propose a three-step sensor placement framework *SoftTouch*- inspired by traditional contact-based approaches [1], [19]- to determine sensor placement for soft and dexterous robotic hands. We illustrate SoftTouch with *The Elliot and Connolly Benchmark* [8] which is a standardized benchmark for evaluating in-hand dexterity. The benchmark evaluates the dexterity of soft robotic hands based on 13 distinct in-hand manipulation patterns derived from observations of multiple human subjects from the Elliot and

Connolly paper [20] using objects selected from the Yale-CMU-Berkeley (YCB) Object Set [21]. These manipulation patterns were chosen because they are focused specifically on dexterous manipulations with objects in the hand. They are tied to motions observed in daily life, and cover the full range of potential in-hand manipulations primitives [8]. The benchmark decomposes manipulation into qualitative- *Success or Failure* - and quantitative- *Translation and Rotation Performance Scores*- component metrics. We then use information embedded in the sensors' data for the above-mentioned state estimation, which we use to center our evaluation of different sensor placements.

II. Related Work

A. Contact Frameworks

Conventionally, sensor placement was determined by first performing the task on the human hand, then transferring results to equivalent locations on the robotic hand. Both Wiener et al. [1] and Mirković and Popović [2] determined sensor placement for intertial and force sensors to be the point of contact between the robotic hand and the object. These techniques were developed for conventional hard robotic systems. Due to the deformable nature of soft robotic hands during grasping and manipulation, the same conclusion might not apply to soft robotic systems. There have also been studies that investigated the effect of the number of sensors on successful grasping [22]. However, none of these studies evaluated other potential sensor placement configurations which could provide better sensing information.

Classifying motion using contact forces from sensors is also not a new concept. Karaku et al. [23] used contact forces to classify movement type (no movement, contact/release) using a multinomial regression model. Funabashi et al. [15] used a Convolutional Neural Network (CNN) to determine the joint angle of next timestep from estimated joint angle of the current timestep. Hogan et al. [24] divided the role of tactile sensing to Control State control, which reacts to binary slip signals; and Object State control which regulates the applied forces on the object to enforce a desired contact mode.

B. Mathematical Frameworks

There are studies that investigated the number of sensors needed and the effect of different number of sensors on a robotic hand [22]. However, mathematical frameworks are often represented as an optimization problem with respect to task-specific manipulations or robot kinematics.

Spielberg et al. [13] optimized for task-specific manipulation by accounting for the deformable nature of soft robotic hands using strain and strain rates. As a result, they determined the optimal sensor placement by assessing expected value of data from a given configuration for object grasping prediction, learned proprioception, and control. Kim et al. [25] instead optimize based on kinematics considerations. They determined sensor placement by setting the constraint on the number of sensors used, and then determine computationally where to place the sensors to minimize shape and tip error between a reconstruction model and a mechanics-based mode. However, both these proposed frameworks were not evaluated on a real robotic hand, but rather left for future exploration. Computational techniques to estimate sensor data are often not reliable enough for real-world tasks [26]. Furthermore, it might be challenging to fit all necessary sensors in limited available space of the simulated optimal configuration [12]. Therefore, we believe that there is value in evaluating different sensor placements on a physical robotic hand.

C. Hand/Sensor Design Frameworks

There are also studies that examine contact forces through wrapping the hand with a sensorized glove. STAG [27], for instance, studies the contact force signatures captured for different types of in-hand manipulations. However, building a custom glove for other types of hands that have different morphology and geometry is not a simple or quick task. On the other hand, Hennig et al. [28] developed a sensor glove that uses fewer sensors placed in frequent contact regions. Hennig and colleagues noticed that there were *undetected grasp attempts*, and attribute this finding to suboptimal sensor placement. This result suggests the need for a sensor placement framework that is evaluated based on key manipulation metrics such that such false negatives can be minimized.

There are also many studies investigating new sensor designs that are complementary for soft systems. DefSense [29] and FingerVision [30] are both deformable sensors that are complementary with soft systems. DIGIT [31] is even designed with the application of dexterous manipulation in mind. However, such sensors are expensive and not easily reconfigurable for different types of soft hand designs.

Our proposed sensor placement framework - SoftTouch - is a contact-inspired framework for highly dexterous soft robotic hands [1], [2]. Our framework evaluates sensor placement on a physical robotic hand performing real-world manipulation tasks [20], [26], based on data collected from sensors placed in a given configuration [23] using state-of-the-art manipulation metrics [8]. The key advantage of our framework lies in its easy reconfigurability for different soft robotic hands, and its complementarity with off-the-shelf sensors without the need to design a new soft hand or skin.

III. SoftTouch Framework

A. 3-Steps Framework

1) **Perform Contact Experiment**
   In this step, a human contact experiment is performed on the 13 manipulation patterns established by Elliot and Connolly [20]. The object used for each manipulation pattern is taken from Table. I.
   First, each of the objects is stained using green paint. Next, the manipulation patterns are performed on the stained objects with a human hand. We present our contact experiment results in Fig. 1. Three manipulation patterns are chosen for further investigation. The equivalent stained locations on the human hand for

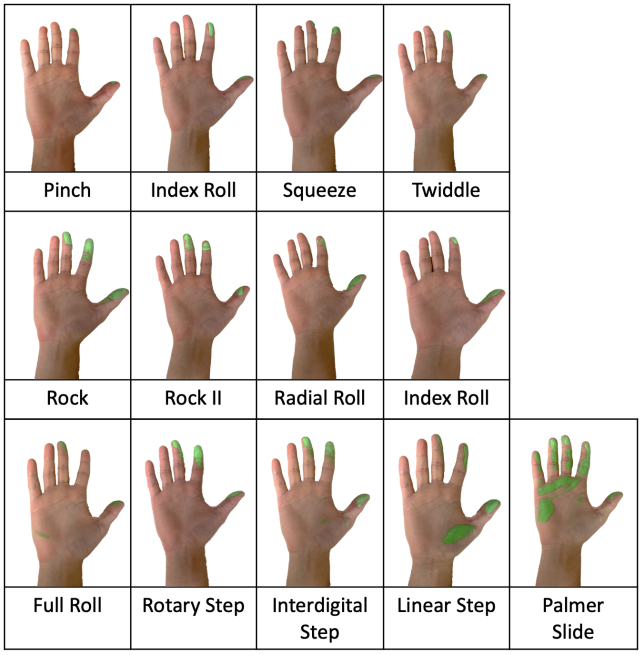

Fig. 1: Results from Contact Experiments. Green stains mark regions that comes in contact when performing the manipulation pattern.

Manipulation Pattern	Object	YCB ID	Metrics
Pinch (P)	Bolt & Nut	46, 47	T_z
Dynamic Tripod (DT)	Small Marker	41	T_z
Squeeze (S)	Syringe	N/A	T_y
Twiddle (T)	Bolt & Nut	46, 47	T_z, R_x
Rock (R)	Cup (yellow)	64	R_z
Rock II (RII)	Small Marker	41	R_y
Radial Roll (RR)	Marble (green)	62	T_z, R_x
Index Roll (IR)	Marble (green)	62	T_z, R_x
Full Roll (FR)	Wood Block	69	R_x
Rotary Step (RS)	Cup (yellow)	64	R_z
Interdigital Step (IS)	Small Marker	41	T_y
Linear Step (LS)	Large Marker	40	T_x
Palmar Slide (PS)	Large Marker	40	R_x

TABLE I: YCB Objects and Metrics for the Elliott and Connolly Benchmark; T- Translation, R- Rotation, subscript represents respective axis for metric.

these three patterns are then marked on a soft robotic hand (Fig. 4).

2) **Identify Candidate Configurations**
Sensor placement configurations where the sensors are not placed at contact locations should also be evaluated. This is because vibrations get propagated to the entire hand. Furthermore, sensors that are placed at a distance away from the manipulation are also less likely to interfere with the manipulation. Therefore, sensors that are not placed exactly at the contact points may be better at picking up information about the manipulation.
We propose identifying candidate configurations comprising sensors placed at contact points identified in the previous step; sensors placed midway between the contact points and the furthest locations from the contact points; and sensors placed at locations furthest from the contact points. While there are many such configurations, we suggest selecting a subset that is most relevant for evaluation while considering the space constraints of the hand . We provide an example and justifications for it in Section V-B.

3) **Evaluate each Configuration**
For each configuration, the soft robotic hand performs selected manipulation patterns [20] on the objects referenced in Table. I. A fiducial marker (AprilTag) which records the translation and rotation along the given axis is attached to each object [8]. For the RockII manipulation, two AprilTags are attached on each end of the pen and the angle of rotation is calculated using trigonometry.
The qualitative metric is determined by observing whether the manipulation was successful. The quantitative metrics can be decomposed into translation distance and angle of rotation [8], which is determined from the motion of the AprilTag. Each configuration is evaluated based on how well the data captured by sensors placed in the given configuration are at predicting these metrics. Given training sensor data, we represent the continuous metric as a univariate or bivariate regression problem and the binary metric as a binary classification problem. A Final Total Score then weighs the performance scores between the regressor and classifier, and the final sensor placement is determined from the configuration with the highest value Section. IV.

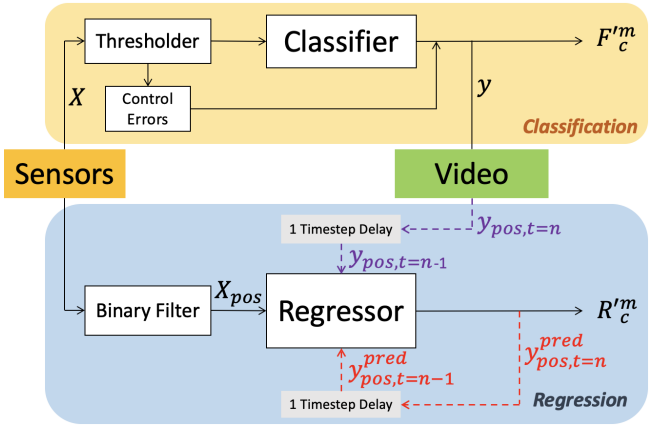

Fig. 2: Flowchart for Classification (SVM) and Regression (Ridge) Models. Regression Model is trained only on successful manipulations represented with Binary Filter. Red dotted arrows are flow targets at test time.

B. Regressor

The current position of the object is a function of current sensor values and previous position. To predict the current position, we can use a regression model. In particular, we chose the Ridge Regression Model (RRM) as we observe better performance compared to Linear Regression in our initial exploration. The regression model is trained on a subset of successful manipulations X_{pos}.

The regression model is visualized in the bottom half of the flowchart in Fig. 2. During training, the regression model takes in the true position of the object at the previous timestep $y_{pos,t=n-1}$ and the sensor data at the current timestep X_{pos} to predict the position at the current timestep $y'_{pos,t=n}$, starting from timestep $n = 0$. During test time, the regression model takes in the predicted position of the previous timestep $y'_{pos,t=n-1}$ and the sensor data at the current timestep X_{pos} to predict the position at the current timestep $y'_{pos,t=n}$.

C. Classifier

A Binary Classifier is trained on the same distribution of sensor data collected from each sensor placement configuration and each type of manipulation pattern. In particular, we chose Support Vector Classifier (SVC) with a linear kernel among other kernels and models such as Random Forest Classifier due to better performance. The distribution X comprises 80% positive class and 20% negative class containing equal distribution of "Control Errors", "Slips" and "No Object". The target y is the binary metric defining whether the manipulation pattern was successful, which is labelled qualitatively from the video.

As shown in the top half of Fig. 2, a threshold is first used to filter out control failures. This threshold is determined from the maximum absolute sensor readings when the robotic hand is at rest. The SVC is then evaluated on the filtered training set with 5 random seeds and a train-test split of 80/20.

IV. Performance Scores

A. Relative Regression Score

The Mean Squared Error (MSE), R'^{m}_{c}, is computed for each manipulation pattern m and given configuration c. R'^{m} represents the set containing the MSE of all the evaluated configurations for a given manipulation pattern. Relative Regression Score, R^{m}_{c}, for each manipulation m and given configuration m is defined as the relative MSE compared to the lowest MSE in the set. This relation can be represented mathematically as follows.

$$R^{m}_{c} = \frac{R'^{m}_{c} - \min(R'^{m})}{\max(R'^{m}) - \min(R'^{m})} \times 100 \tag{1}$$

If the manipulation can be defined by both translation and rotation scores, R^{m}_{c} is the average of the Relative Translation and Relative Rotation Regression Scores.

B. Relative Classification Score

Since the Relative Regression Score is computed relative to the other configurations of a given manipulation pattern, the Classification Score should also be relative to the other configurations in order to make a fair comparison between the classification and regression performance.

The Classification Score, F'^{m}_{c}, for each manipulation pattern m and given configuration c is the accuracy score out of 100%. F'^{m} represents the set containing the Classification Scores of all the evaluated configurations for a given manipulation pattern. Relative Classification Score, F^{m}_{c}, for each manipulation m and given configuration c is defined as the relative classification score compared to the lowest classification score in the set F'^{m}. This relation can be represented mathematically as follows.

$$F^{m}_{c} = \frac{F'^{m}_{c} - \min(F'^{m})}{\max(F'^{m}) - \min(F'^{m})} \times 100 \tag{2}$$

C. Total Final Score (T)

T^{m}_{c} condenses the Relative Classification and Regression Scores into a single performance score for a given manipulation pattern and configuration

$$T^{m}_{c} = \alpha \times F^{m}_{c} + (1 - \alpha) \times R^{m}_{c} \mid 0 \leq \alpha \leq 1 \tag{3}$$

where α is the weighted importance between the classification and regression performance scores. The coefficient α is dependent on application, but we use $\alpha = 0.5$ for simplicity. The best sensor placement for a given manipulation pattern is therefore the configuration that leads to the highest T^{m}_{c}.

V. Experiments

A. Setup

The SoftTouch framework was completed with the CMU Foam Hand III [8], a bio-inspired, tendon-driven dexterous robotic hand made almost entirely of foam. It has a high level of dexterity while requiring a relatively low number of motors (10) for operation.

For our experiments, we evaluated on 2 off-the-shelf sensors- MPU9250 Inertial Measurement Unit (IMU) and Taidacent Force Sensitive Resistor (FSR)- due to their easy reconfigurability on different soft robotic hands. A 5MP Raspberry Pi Zero W camera module was placed $35\,\mathrm{cm}$ away from the hand to record each manipulation. The camera was calibrated with the standard 7x7 checkerboard to get the intrinsic camera parameters used to process the translation and the rotation of the AprilTag. The sensors were sampled at a rate of 84Hz, while the camera was sampled at the standard 30fps. We tested our framework on a subset of 3 manipulation patterns- Dynamic Tripod, Rock II and Index Roll. These patterns represent all 3 possible combinations of the quantitative metrics (Translation and Rotation) described in Table. I. The keyframes for a successful manipulation of these patterns are shown in Fig. 3.

B. Hand-To-Robot Conversion

Given the size of the sensors used and the space constraints on the CMU Foam Hand III, we define the mapping between the human hand and the soft robotic hand in Fig. 4. As described in the Section. III, the contact experiments for the three experiments were first performed (Fig. 1). We then selected 4 distinct configurations to evaluate as shown in Fig. 5 (right) on the two sensors (IMUs and FSRs).

Configuration $A1$ represents the configuration following traditional contact-inspired frameworks on rigid robot hands. In this configuration, all the sensors are placed at contact points. We hypothesize that the configuration $A1$ leads to the

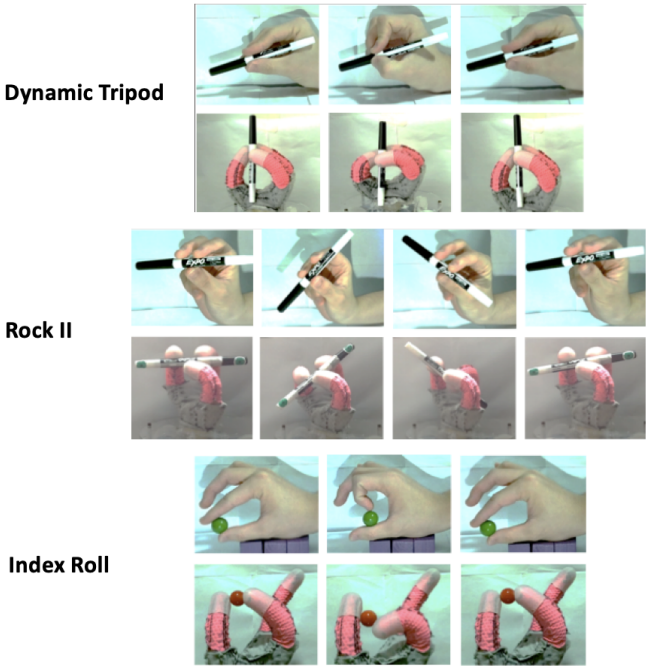

Fig. 3: Key Frames of Successful Manipulations on Human and Robotic Hands.

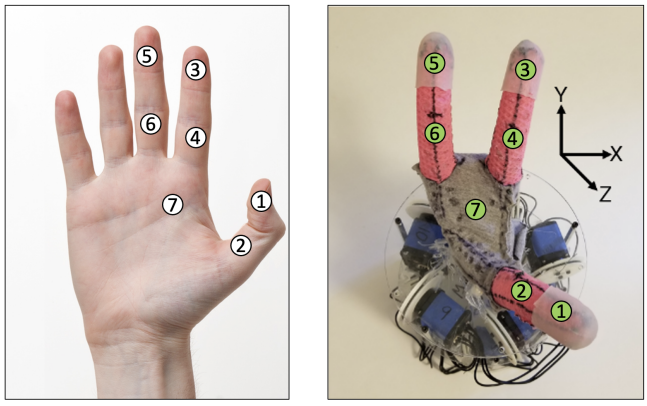

Fig. 4: One-to-One Mapping between Human Hand and Soft Robotic Hand. Position 7 represents the furthest point from the contact points.

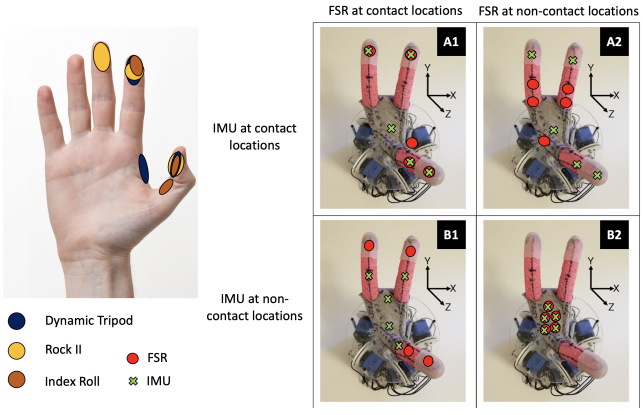

Fig. 5: Marked contact points on the human hand (left) Selected Sensor Placement Configurations (right).

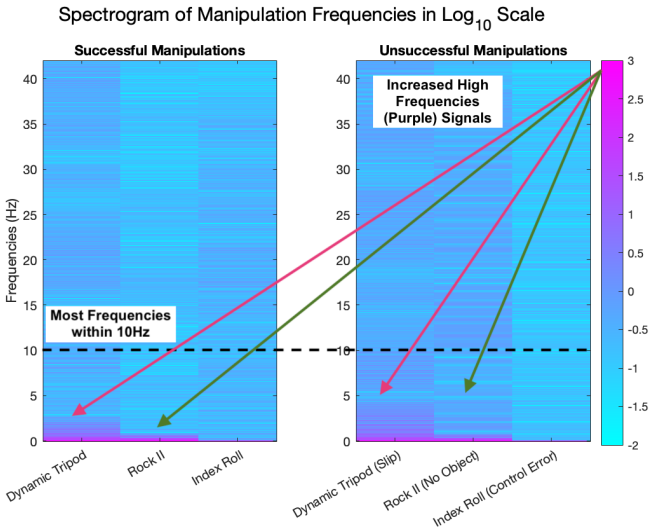

Fig. 6: Spectrogram of Successful (left) and Unsuccessful (right) manipulation patterns

best Final Total Score based on the conclusion reached by earlier studies on conventional rigid hands [1], [2]. Configuration $B2$ serves as a baseline for the other configurations. At this configuration, all the sensors are placed furthest away from contact points. We also hypothesize that configuration $B2$ leads to the lowest Final Total Score, since all the sensors are placed furthest away from the contact points and therefore receives the weakest signals. Configuration $B1$ and $A2$ both represent configurations where sensors are placed midway between the contact points and the furthest locations from the contact points. In particular, $B1$ represents the configuration where the IMUs are placed at the midpoint, but the FSRs are placed at the contact points. $A2$ represents the configuration where the FSRs are placed at the midpoint, but the IMUs are placed at the contact points. The results of these configurations are compared with $A1$ to determine if sensors placed at non-contact locations can pick up signals that are best for manipulation task metrics. The sensors were also securely fastened to the soft hand with both threads and masking-tapes to minimize unintended movement in the IMU during the manipulation.

C. Data Processing

We refer to each manipulation pattern conducted as a "run". The hand is initially at rest at the start of the manipulation. For each run, we first subtract the initial bias at rest. Since the accelerometer will always record the gravitational acceleration, the resulting acceleration vector in the dataset therefore represents the direction and magnitude with respect to the initial gravitational vector. Next, we trim each run to keep only the duration when the manipulation is performed. Since the hand is initially at rest, the start of the manipulation can be determined reliably as the first spike that is recorded by the IMU. Each manipulation took approximately 2.5s. This corresponds to segment containing 210 and 75 samples after the first spike recorded by the IMU and Camera (translation and rotation) respectively. The time

segment for the FSR is the same as the IMU given that they are sampled at the same frequency.

Our experiments show that most frequencies of both the successful and unsuccessful manipulation for the three patterns are contained within 10Hz (Fig. 6). We apply a low pass filter to the IMU data by averaging every 7 samples. For the camera data (translation and rotation), we resample to 90Hz and apply a low pass filter by averaging every 3 samples. Both filters create a cutoff frequency $\approx 10Hz$, and we refer to each of the 30 samples after the averaging as a timestep n. For the classifier, we compute the percentage of time that FSRs are in contact with the object and append this vector with the IMU vector to form X. For the regression model, we compute for each time interval a binary value that represents any FSRs contact during the timestep, and append this vector with the IMU vector to form X_{pos}.

VI. Results And Discussion

The results for the performance scores are illustrated in the Fig. 7. The Final Total Score is computed with $\alpha = 0.5$. The results for $B2$ are not shown as it has a consistent value of 0 across all the performance scores. We conclude that the optimal sensor placement configuration is $A2$ for Dynamic Tripod, $B1$ for Rock II, and $A1$ for Index Roll on the CMU Foam Hand III. If one configuration had to be chosen for all three manipulation tasks, $A2$ would provide the best results, as it is the configuration with the highest minimum performance over all tasks. Given that the framework can be used for other soft hands, manipulations and sensors, the same conclusion might not be reached when some of these variables are changed. However, the tests are straightforward to run for any new sensor, hand, and task suite.

To allow other researchers to apply our sensor placement framework on other sensors, hand designs and task suites, we provide our code for data processing, apriltag detection, and classification and regression modelling [1].

A. Key Takeaways

There are four key takeaways from our results. Firstly, our results confirm that for soft and dexterous robotic hands, sensor placement can affect the quality of sensor data used to estimate the manipulation metrics. This can be seen from Fig. 7 where configurations $A1, B1, A2$ have higher Final Total Score as compared to the configuration $B2$ where all the sensors are placed furthest away from contact points. Furthermore, since the performance scores are different for different configurations, a sensor placement framework is important to select the best configuration for *a given manipulation pattern.*

Secondly, our results suggest that the optimal sensor placement can be different for different manipulations. In the cases of Dynamic Tripod and Rock II, sensors placed at contact points do not always lead to better performance. We notice that IMUs placed at contact locations can affect the quality of some manipulation patterns due to the added weight to the soft and light robotic hands. This manifested for the Rock II pattern where IMUs placed at contact points has lower Relative Regression Score as compared to $A1$ and $A2$. This means that unlike conventional rigid hands, sensors placed at non-contact locations can lead to better estimation of quantitative manipulation metrics. This highlights the need for a proper sensor placement framework to evaluate different placements for *different manipulation patterns*.

Thirdly, our results show that IMUs placed at contact locations leads to higher Relative Classification Scores. This is likely because IMUs placed at contact locations are more sensitive to signals inherent in unsuccessful manipulations. From Table. II, IMUs placed at contact locations tend to predict "Slip" and "No Object" as an unsuccessful manipulation better than when they are placed at non-contact locations (bold red). When the object "Slip(s)", the IMUs pick up a distinct high frequency spike (Ref to Fig. 6). When there is no object in the hand, the fingers move in a different trajectory as compared to the when there is an object in the hands. IMUs placed at contact locations are more sensitive to these small differences. We do observe that across the configurations, "Control Errors" are consistently correctly predicted as they are filtered away by the thresholder (Fig. 2) and are not involved in training.

Lastly, our results show that qualitative information about the manipulation can be detected even at distant locations. This can be seen from Table. II, where even for configuration $B2$, unsuccessful manipulations are often predicted correctly. This is likely due to the fact that the soft robotic hand is a single piece of deformable material. Therefore, the vibrations that carry information about the manipulation can propagate to distant locations on the soft hand.

B. Limitations

Step 1 of our framework requires observed contact regions to be transferred from human to robot hand. While this step may be trivial for anthropomorphic or bioinspired hands such as ours, it can also be performed on non-anthropomorphic hand designs with a map between the Human-To-Robot Hand (Fig. 4).

Our framework is designed under the assumption that the manipulation patterns can be performed on the soft robotic hand. In particular, CMU Foam Hand III can only perform 10 out of the 13 manipulation patterns. The 3 manipulation patterns that we evaluated were a subset that is representative of these 10 successful patterns. However, we believe that this is a reasonable assumption given that it is irrelevant to sensorize a robotic hand that can never perform the manipulation pattern. Therefore, our framework is designed specifically for manipulation patterns that can be performed.

Our framework determines sensor placement by comparing the different sensor configurations. Therefore, we chose to use relative scores to rank the performance of different sensor configurations. Furthermore, relative scores projects regression and classification to the same scale which makes it easier for the experimenter to decide whether more emphasis should be placed on classification or regression. However,

[1] https://github.com/spartace98/SoftTouch

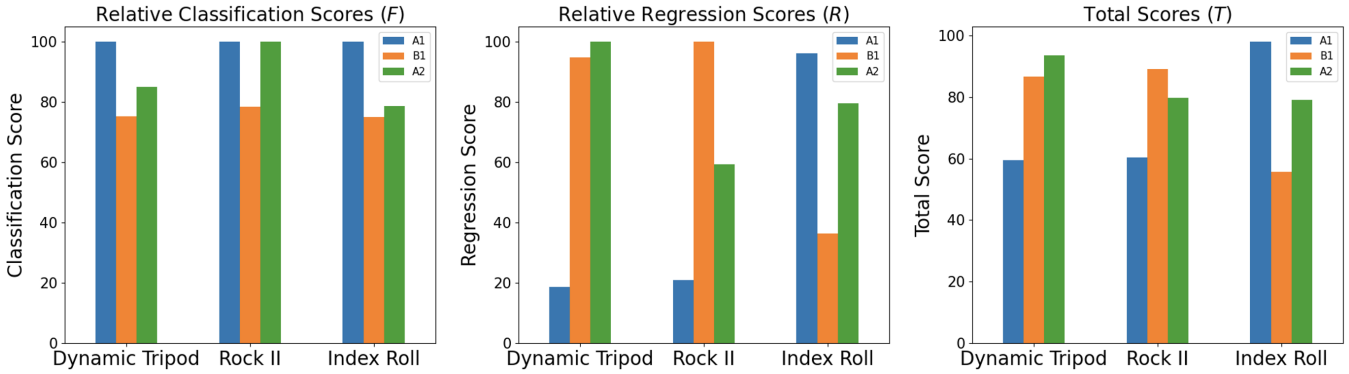

Fig. 7: Summary of Performance Scores for chosen configurations and manipulation patterns- Relative Classification Score (left), Relative Regression Score (middle) and Final Total Score (right). A relative score of 100 indicates highest score in the set of evaluated configurations. Results for $B2$ is not displayed as it has a value of 0 consistently across all performance scores.

		FSR Placement						
		1	2	1	2	1	2	
IMU Placement	A	100.0	100.0	100.0	100.0	100.0	100.0	Control Error
	B	100.0	100.0	100.0	100.0	100.0	100.0	
	A	100.0	66.7	100.0	100.0	100.0	100.0	Slip
	B	66.7	**11.1**	100.0	**55.6**	33.3	**11.1**	
	A	100.0	100.0	100.0	100.0	100.0	50.0	No Object
	B	80.0	**40.0**	100.0	90.0	90.0	**50.0**	
		Dynamic Tripod		Rock II		Index Roll		

TABLE II: Breakdown of Classification Accuracy(%) for Unsuccessful Manipulations. "Control Errors" are unperformed manipulations; "Slips" are manipulations where the object slips out of the hand; "No Object" are performed manipulations without the object in hand; Classification accuracy for chance is 20%, so patterns with values $> 20\%$ are greater than chance.

we do note that relative comparisons are less effective if none of the configurations generate useful data that can be used in classification and regression tasks. Therefore, the experimenter should also account for absolute performance scores when determining the final sensor placement, which we report in our repository.

During our experiments, we observed that when FSRs were attached to the contact points in configurations $A1$ and $B1$, the manipulation was much harder to perform. This is due to the fact that FSRs typically have smooth surfaces and a rigid structure that differs from the natural compliance of the soft hand. As a result, this led to an increase in the number of instances where the object slips out of the hand before and when the manipulation pattern was performed. To resolve the problem of surface roughness, we investigated using a rubber casing to enclose the FSRs. However, this led to an increase in the randomness in the contact sensed, which was recorded as spikes. We also observed that when the Force Sensor readings were removed from the training data, there was no significant change in the performance. This led us to conclude that attaching these specific force sensors might not be a feasible approach to sensoring a soft hand and reinforces the importance of ongoing research towards deformable off-the-shelf force sensors.

C. Future Work

Our study did not test the proposed configuration with a feedback control loop. Given that the eventual goal is to develop autonomous hands that can perform complex in-hand manipulation, we believe that further exploration may be needed to expand our framework to a closed-loop control setting.

Our experiments also did not evaluate mixed sensor configurations where sensors are placed at both contact and non-contact locations. Earlier studies have reported that greater sensor coverage at both contact and non-contact points can lead to improved performance of the full pre- and post-contact policy [22]. Therefore, we believe further exploration is needed to assess these mixed configurations.

Given that our framework is designed to reduce complexity in sensor placement decision making, we propose using classical machine learning techniques that can generate the performance scores quickly. We eventually converged on using RMM and SVC as they generated the highest performance scores which indicates a strong relationship between sensor data and the manipulation metrics. Deep learning neural networks can possibly generate higher performance scores, which we leave as future work.

Finally, we look forward to testing our framework with other sensors.

VII. Conclusion

This paper proposes a sensor placement framework for a highly dexterous soft robotic hand. Our framework directly assesses different sensor placements with a physical robotic hand based on state-of-the-art qualitative and quantitative manipulation metrics. The key advantage of our framework lies in its easy reconfigurablity to different soft robotic hands and off-the-shelf sensors. We also presented results for experiments conducted using the framework. Our results showed

that even for soft and dexterous hands, sensor placement can affect the quality of the data collected. Furthermore, we showed that similar to rigid hands, sensors sometimes perform best when they are placed at contact points. However, this finding was not universal, and placing sensors away from contact points sometime led to better results, especially for estimating quantitative manipulation metrics.

ACKNOWLEDGEMENT

Thanks to Ryan Coulson (CMU) for his contribution to the CMU Foam Hand III. This research was partially supported by NSF award CMMI-1925130 and by the AI Research Institutes program supported by NSF and USDA-NIFA under AI Institute for Resilient Agriculture, Award No. 2021-67021-35329. Chao Li was supported by CMU Summer Undergraduate Research Fellowship and Small Undergraduate Research Grant.

REFERENCES

[1] Pascal Weiner, Caterina Neef, Yoshihisa Shibata, Yoshihiko Nakamura, and Tamim Asfour. An embedded, multi-modal sensor system for scalable robotic and prosthetic hand fingers. *Sensors*, 20(1), 2020.

[2] Bojana Mirkovic and Dejan Popović. Prosthetic hand sensor placement: Analysis of touch perception during the grasp. *Serbian Journal of Electrical Engineering*, 11:1–10, 01 2014.

[3] Balakumar Sundaralingam, Alexander Sasha Lambert, Ankur Handa, Byron Boots, Tucker Hermans, Stan Birchfield, Nathan Ratliff, and Dieter Fox. Robust learning of tactile force estimation through robot interaction. In *2019 International Conference on Robotics and Automation (ICRA)*, pages 9035–9042, 2019.

[4] Jonathan P King, Dominik Bauer, Cornelia Schlagenhauf, Kai-Hung Chang, Daniele Moro, Nancy Pollard, and Stelian Coros. Design. fabrication, and evaluation of tendon-driven multi-fingered foam hands. In *2018 IEEE-RAS 18th International Conference on Humanoid Robots (Humanoids)*, pages 1–9. IEEE, 2018.

[5] Cornelia Schlagenhauf, Dominik Bauer, Kai-Hung Chang, Jonathan P King, Daniele Moro, Stelian Coros, and Nancy Pollard. Control of tendon-driven soft foam robot hands. In *2018 IEEE-RAS 18th International Conference on Humanoid Robots (Humanoids)*, pages 1–7. IEEE, 2018.

[6] Dominik Bauer, Cornelia Bauer, Jonathan P King, Daniele Moro, Kai-Hung Chang, Stelian Coros, and Nancy Pollard. Design and control of foam hands for dexterous manipulation. *International Journal of Humanoid Robotics*, 17(01):1950033, 2020.

[7] Bianca S Homberg, Robert K Katzschmann, Mehmet R Dogar, and Daniela Rus. Robust proprioceptive grasping with a soft robot hand. *Autonomous robots*, 43(3):681–696, 2018.

[8] Ryan Coulson, Chao Li, Carmel Majidi, and Nancy S. Pollard. The elliott and connolly benchmark: A test for evaluating the in-hand dexterity of robot hands. In *2020 IEEE-RAS 20th International Conference on Humanoid Robots (Humanoids)*, pages 238–245, 2021.

[9] Yu She, Chang Li, Jonathon Cleary, and Hai-Jun Su. Design and Fabrication of a Soft Robotic Hand With Embedded Actuators and Sensors. *Journal of Mechanisms and Robotics*, 7(2), 05 2015. 021007.

[10] Jianshu Zhou, Xiaojiao Chen, Ukyoung Chang, Jui-Ting Lu, Clarisse Ching Yau Leung, Yonghua Chen, Yong Hu, and Zheng Wang. A soft-robotic approach to anthropomorphic robotic hand dexterity. *IEEE Access*, 7:101483–101495, 2019.

[11] Jun Shintake, Vito Cacucciolo, Dario Floreano, and Herbert Shea. Soft robotic grippers. *Advanced Materials*, 30(29):1707035, 2018.

[12] Aude Billard and Danica Kragic. Trends and challenges in robot manipulation. *Science*, 364(6446):eaat8414, 2019.

[13] Andrew Spielberg, Alexander Amini, Lillian Chin, Wojciech Matusik, and Daniela Rus. Co-learning of task and sensor placement for soft robotics. *IEEE Robotics and Automation Letters*, 6(2):1208–1215, 2021.

[14] Ziwei Xia, Zhen Deng, Bin Fang, Yiyong Yang, and Fuchun Sun. A review on sensory perception for dexterous robotic manipulation. *International Journal of Advanced Robotic Systems*, 19(2):17298806221095974, 2022.

[15] Satoshi Funabashi, Tomoki Isobe, Fei Hongyi, Atsumu Hiramoto, Alexander Schmitz, Shigeki Sugano, and Tetsuya Ogata. Multi-fingered in-hand manipulation with various object properties using graph convolutional networks and distributed tactile sensors. *IEEE Robotics and Automation Letters*, 7(2):2102–2109, 2022.

[16] Jianshu Zhou, XiaoJiao Chen, Ukyoung Chang, Jia Pan, Wenping Wang, and Zheng Wang. Intuitive control of humanoid soft-robotic hand bcl-13. In *2018 IEEE-RAS 18th International Conference on Humanoid Robots (Humanoids)*, pages 314–319, 2018.

[17] OpenAI: Marcin Andrychowicz, Bowen Baker, Maciek Chociej, Rafal Józefowicz, Bob McGrew, Jakub Pachocki, Arthur Petron, Matthias Plappert, Glenn Powell, Alex Ray, Jonas Schneider, Szymon Sidor, Josh Tobin, Peter Welinder, Lilian Weng, and Wojciech Zaremba. Learning dexterous in-hand manipulation. *The International Journal of Robotics Research*, 39(1):3–20, 2020.

[18] J. Sun, J. King, and N. Pollard. Characterizing continuous manipulation families for dexterous soft robot hands. *Frontiers in robotics and AI*.

[19] Hiroaki Hasegawa, Yoshitomo Mizoguchi, Kenjiro Tadakuma, Aiguo Ming, Masatoshi Ishikawa, and Makoto Shimojo. Development of intelligent robot hand using proximity, contact and slip sensing. In *2010 IEEE International Conference on Robotics and Automation*, pages 777–784, 2010.

[20] John M Elliott and KJ Connolly. A classification of manipulative hand movements. *Developmental Medicine & Child Neurology*, 26(3):283–296, 1984.

[21] Berk Calli, Aaron Walsman, Arjun Singh, Siddhartha Srinivasa, Pieter Abbeel, and Aaron M Dollar. Benchmarking in manipulation research: The ycb object and model set and benchmarking protocols. *arXiv preprint arXiv:1502.03143*, 2015.

[22] Michael C. Koval, Nancy S. Pollard, and Siddhartha S. Srinivasa. Pre- and post-contact policy decomposition for planar contact manipulation under uncertainty. *The International Journal of Robotics Research*, 35(1-3):244–264, 2016.

[23] İpek Karakuş, Hasan Şahin, Ahmet Atasoy, Erkan Kaplanoğlu, Mehmed Özkan, and Burak Güçlü. Evaluation of sensory feedback from a robotic hand: A preliminary study. In Domenico Prattichizzo, Hiroyuki Shinoda, Hong Z. Tan, Emanuele Ruffaldi, and Antonio Frisoli, editors, *Haptics: Science, Technology, and Applications*, pages 452–463, Cham, 2018. Springer International Publishing.

[24] Francois R. Hogan, Jose Ballester, Siyuan Dong, and Alberto Rodriguez. Tactile dexterity: Manipulation primitives with tactile feedback. In *2020 IEEE International Conference on Robotics and Automation (ICRA)*, pages 8863–8869, 2020.

[25] Beobkyoon Kim, Junhyoung Ha, Frank C. Park, and Pierre E. Dupont. Optimizing curvature sensor placement for fast, accurate shape sensing of continuum robots. In *2014 IEEE International Conference on Robotics and Automation (ICRA)*, pages 5374–5379, 2014.

[26] Qian Wan, Ryan P. Adams, and Robert D. Howe. Variability and predictability in tactile sensing during grasping. In *2016 IEEE International Conference on Robotics and Automation (ICRA)*, pages 158–164, 2016.

[27] Subramanian Sundaram, Petr Kellnhofer, Yunzhu Li, Jun-Yan Zhu, Antonio Torralba, and Wojciech Matusik. Learning the signatures of the human grasp using a scalable tactile glove. *Nature*, 569(7758), 2019.

[28] Robert Hennig, Jessica Gantenbein, Jan Dittli, Haotian Chen, Stéphanie P. Lacour, Olivier Lambercy, and Roger Gassert. Development and evaluation of a sensor glove to detect grasp intention for a wearable robotic hand exoskeleton. In *2020 8th IEEE RAS/EMBS International Conference for Biomedical Robotics and Biomechatronics (BioRob)*, pages 19–24, 2020.

[29] Moritz Bächer, Benjamin Hepp, Fabrizio Pece, Paul G. Kry, Bernd Bickel, Bernhard Thomaszewski, and Otmar Hilliges. Defsense: Computational design of customized deformable input devices. In *Proceedings of the 2016 CHI Conference on Human Factors in Computing Systems*, CHI '16, page 3806–3816, New York, NY, USA, 2016. Association for Computing Machinery.

[30] Akihiko Yamaguchi and Christopher G. Atkeson. Implementing tactile behaviors using fingervision. In *2017 IEEE-RAS 17th International Conference on Humanoid Robotics (Humanoids)*, pages 241–248, 2017.

[31] Mike Lambeta, Po-Wei Chou, Stephen Tian, Brian Yang, Benjamin Maloon, Victoria Rose Most, Dave Stroud, Raymond Santos, Ahmad Byagowi, Gregg Kammerer, Dinesh Jayaraman, and Roberto Calandra. Digit: A novel design for a low-cost compact high-resolution tactile sensor with application to in-hand manipulation. *IEEE Robotics and Automation Letters*, 5(3):3838–3845, 2020.